remote sensing

MDPI

Article

Uncovering Forest and Cropland Change with High-Resolution Data in a Biodiversity Hotspot, Madagascar

Zy Harifidy Rakotoarimanana [1,*], Nobuhito Ohte [1] and Zy Misa Harivelo Rakotoarimanana [2]

[1] Graduate School of Informatics, Kyoto University, Yoshida-Honmachi, Sakyo-ku, Kyoto 606-8501, Japan
[2] Sosyal Bilimler Enstitüsü, Dokuz Eylül Üniversitesi, Tınaztepe Yerleşkesi, Buca 35390, İzmir, Turkey
* Correspondence: zy.harifidy.27f@st.kyoto-u.ac.jp

Highlights

What are the main findings?

- Forest cover stayed under 8.5% in Betsiboka, over 34.6% in ANP; cropland remained below 7%. High accuracy in both regions (OA = 0.87–0.95), with stronger datasets agreement in ANP than Betsiboka (Kappa = 0.68–0.90).
- FROM-GLC10 and ESA best for cropland in Betsiboka; DW and ESRI best for forest, especially in ANP. By 2100, forests may rise 230–300% in Betsiboka but drop up to 39% in ANP across SSPs.

What is the implication of the main finding?

- We assess past and future forest and cropland changes in the Betsiboka basin and the ANP.
- This study highlights the importance of high-resolution ground-based land use data for monitoring land management and calibrating a hydrological model in the region.

Abstract

The lack of reliable methods for cropland and forest monitoring remains a challenge in the Betsiboka basin and Ankarafantsika National Park (ANP), Madagascar. A key novelty of our study is the comparative analysis of multiple high-resolution datasets for 2017 and 2021 and future projections under five Shared Socioeconomic Pathways (SSPs) from 2020 to 2100 using Google Earth Engine and Python. Results indicate that forest cover has remained below ~9% in the Betsiboka basin and above ~35% in ANP, while cropland stays under 7% in both areas. Inter-dataset agreement showed high overall accuracy (OA = 0.87–0.95), with stronger agreement in ANP (Kappa = 0.68–0.90). FROM-GLC10 and ESA performed best for cropland classification in Betsiboka, while Dynamic World and ESRI were most accurate for forest, particularly in ANP. Projections suggest that by 2100, forest area in Betsiboka may increase by +230% under SSP3 and +300% under SSP5, whereas ANP could see declines up to 39% under SSP1, −2.2% SSP5, and −1.4% SSP3. The predicted minor cropland increase across both regions suggests that forest expansion is unlikely to significantly constrain agricultural land, illustrating the potential for sustainable intensification and agroforestry to address food security challenges.

Keywords: forest; cropland; high-resolution; remote sensing; Betsiboka basin; Ankarafantsika National Park

check for updates

Academic Editor: Carmine Serio

Received: 6 September 2025
Revised: 27 September 2025
Accepted: 11 October 2025
Published: 15 October 2025

Citation: Rakotoarimanana, Z.H.; Ohte, N.; Rakotoarimanana, Z.M.H. Uncovering Forest and Cropland Change with High-Resolution Data in a Biodiversity Hotspot, Madagascar. *Remote Sens.* **2025**, *17*, 3441. https://doi.org/10.3390/rs17203441

Copyright: © 2025 by the authors. Licensee MDPI, Basel, Switzerland. This article is an open access article distributed under the terms and conditions of the Creative Commons Attribution (CC BY) license (https://creativecommons.org/licenses/by/4.0/).

1. Introduction

Reliable methods and data for monitoring cropland dynamics and forest cover change remain urgent challenges in the Betsiboka basin and Ankarafantsika National Park, Madagascar. Accurate land use land-cover (LULC) data are essential for effective hydrological modeling in these regions [1]. Recent advances in remote sensing and machine learning have led to the development of high-resolution global LULC datasets [2,3]. Multiple global and regional land cover datasets exist, each with different classification schemes, spatial resolutions, and accuracy levels [4]. A variety of high-resolution LULC datasets are available at 10 m, including ESA WorldCover [5], Esri Land Cover [6], Google Dynamic World [7], and FROM_GLC10 [8]. Several studies compared these datasets at the global level [9–11], in Southeast Asia [12], in Africa [13], and in Madagascar [14].

Understanding past and future land cover changes is essential for sustainable land use planning under climate and socioeconomic shifts. Several high-resolution datasets have been employed for this purpose, each with distinct strengths and limitations. While ESA WorldCover dataset provides globally consistent annual land cover maps but lacks the temporal frequency needed for rapid monitoring, where Google Dynamic World excels with near-daily updates, albeit with higher uncertainty under persistent cloud cover [5,7]. Esri Land Cover stands out for its seamless integration with ArcGIS and user-friendly accessibility, though it can misclassify heterogeneous landscapes, while FROM_GLC10, despite being slower to update, provides robust historical baselines and demonstrates strong accuracy in Asia and developing regions [6,8]. For example, ESRI has been applied to track deforestation and cropland changes in East Africa [15]. However, some studies note misclassification issues in heterogeneous landscapes, such as savannas [16]. ESA WorldCover has supported studies on wetland loss in South Sudan and agricultural land use [17]. FROM-GLC10 remains challenging in arid and semi-arid regions of Africa due to spectral confusion between bare soil and sparse vegetation [18]. Despite this, it has been used in regional studies like in Madagascar [19]. Dynamic World dataset has been used to assess post-disaster land cover changes in Mozambique and seasonal agriculture [7].

Despite the proliferation of these global products, their performance and consistency in complex, heterogeneous, and data-scarce regions like Madagascar remain poorly understood, particularly for monitoring cropland. Madagascar is highly biodiverse but threatened by human activities [20]. The Betsiboka basin and the Ankarafantsika National Park (ANP) represent a critical ecosystem facing rapid environmental change, including deforestation and soil erosion [21,22]. Despite extensive research on deforestation using global land datasets in Madagascar, a critical gap remains in understanding the dynamics of cropland expansion, a key factor in ensuring food security for the country. Moreover, this region is home to numerous endemic species and provides essential resources for local communities [23,24]. However, the lack of high-resolution local land use poses a challenge for monitoring the basin and setting a hydrological model. For instance, Raharimahefa & Kusky (2010) used low spatial multitemporal satellite data (30 m resolution) to monitor the changes in sediment transport in the Bombetoka Bay and the Betsiboka estuary [25]. Our previous study used ESRI and ESA global land cover datasets at 300 m resolution to assess the land use change across the major river basins in Madagascar [1]. However, incorporating high-resolution land use offers the potential to significantly enhance hydrological modeling. A recent study assessed the agreement of different global satellite forest monitoring datasets in Madagascar by resampling them all to a 30 m resolution. Their study revealed that the levels of agreement between global land use datasets varied by forest type and region. High disagreement levels were found in dry forest ecosystems between 2016 and 2020 [14]. The Betsiboka basin has an arid climate, which is why we evaluated the accuracy of these high-resolution global datasets in this region. Rafanoha-

rana et al. (2024) projected the forest cover change in 2050 and its implications for lemur conservation in Madagascar's protected areas [24]. However, they highlighted the need to refine deforestation predictions by incorporating dynamic factors and improving remote sensing accuracy. Limited information was demonstrated to affect land model accuracy and distribution maps [20,26].

Our study addresses this by assessing the historical and future change in forest and cropland in the Betsiboka basin and ANP. This paper compares four high-resolution (10 m) global land cover datasets to assess their consistency in classifying forest and cropland for the years 2017 and 2021. We also analyze the changes in LULC under different future climate scenarios using a high-resolution (1 km grid) global dataset. The future analysis particularly focuses on deforestation, cropland expansion, and land cover transitions under different Shared Socioeconomic Pathways (SSPs) scenarios between 2020 and 2100. This multi-dataset approach is particularly novel in the context of Madagascar, where such cross-comparison at high resolution has not been systematically conducted.

The present study examines four primary research questions:

1. Where do these datasets show greatest spatial agreement?
2. Which land cover classes exhibit the most disagreement?
3. Which datasets are suitable for monitoring the forest and cropland in the Betsiboka basin and ANP?
4. What implications does this have for environmental monitoring in the region?

2. Materials and Methods

2.1. Study Area

The study area (Figure 1) covers the Betsiboka basin (55,689 km^2) and ANP (1350 km^2) in northwest Madagascar. This region is characterized by a hot climate with a pronounced dry season. ANP, for example, receives an annual average precipitation of about 1615 mm, which is concentrated in a few months, and a mean temperature of about 26.1 °C [27]. The Betsiboka River has supported the Marovoay rice plain by providing essential irrigation in northwestern Madagascar. However, water flow is projected to decrease by 2100 [28], which may reduce irrigation capacity and, in turn, affect future agricultural land use. The Betsiboka basin was identified as one of the water-stressed basins projected to face scarcity by 2050 [29]. Reduced water availability could constrain irrigation and alter cropping practices, thereby influencing future LULC trajectories. ANP is a significant site within Madagascar's unique biodiversity landscape, serving as a critical area for conservation and research. Despite its ecological importance, ANP faces environmental degradation including fire [30], deforestation [31], and unsustainable agricultural practices [32]. The region is covered by three principal ecotypes including mangrove forests (23%), alluvial agricultural zones (41%), and dry deciduous woodlands (36%). While these land-cover categories reflect current land use, the natural vegetation of the region is largely grassland formations, typically described as savannahs or steppes.

2.2. Data Processing

This study compared five high-resolution global land cover datasets (Table 1) across the Betsiboka basin and ANP.

We selected these four 10 m datasets because they represent the most recent, globally available, high-resolution, broad use and validation in recent peer-reviewed studies. The LULC datasets indeed differ in temporal coverage. To address this, we selected the closest available year for each dataset within or near our study period (2017–2021). This approach minimizes the risk of bias from short-term interannual fluctuations. This analysis was conducted in Google Earth Engine (GEE) and Python 3.11.11. All code is archived

with a DOI [https://doi.org/10.5281/zenodo.16598166] for full reproducibility to other basins. Figure 2 illustrates the workflow diagram for historical land use assessment in the study area.

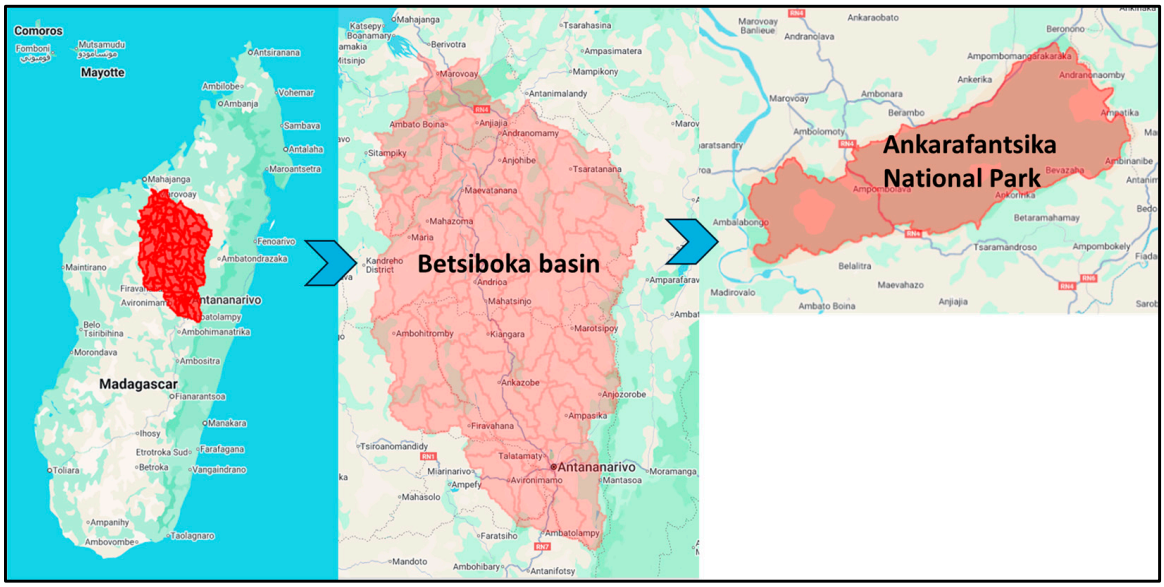


Figure 1. Map of the study area.

Table 1. Description of the datasets.

	Global LULC Datasets	Forest Class ID	Cropland Class ID	Input Data	Classification Method and Accuracy	Data Source
Historical LULC 10 m resolution	FROM_GLC10 (2017)	2	1	Sentinel-2, Landsat	Random Forest (72.8%, Global)	Gong et al. (2019) [8]
	ESRI Land Cover (2017–2023)	2	4	Sentinel-2, AI	Deep Learning (UNet) (85%, Global)	Karra et al. (2021) [6]
	ESA WorldCover (2020, 2021)	10	40	Sentinel-1 and Sentinel-2	Machine Learning (74.4%, Global)	Zanaga et al. (2022) [5]
	DynamicWorld (2015–Present)	1	1	Sentinel-2 + AI	Probabilistic NN (77.5%, Global)	Brown et al. (2022) [7]
Future LULC 1 km grid resolution	Global LULC Projection Dataset under SSP-RCP Scenarios at 1 km Resolution (2020–2100)	2	1	ESA-CCI historical LULC data	GCAM model and cellular automata model-PLUS (Kappa = 0.94, OA = 0.97, FoM = 0.10)	Zhang et al. (2023) [33]

The data loading and reclassification process began with each dataset being imported using GEE and a Python library specialized in geospatial raster data. All historical datasets were originally at a uniform 10 m resolution, so there was no need for resampling. Each dataset was then spatially subsetted to focus on the Betsiboka basin and ANP boundaries by masking with shapefiles and aligning the spatial extent. All rasters were reprojected to EPSG:32738 (UTM Zone 38S), ensuring that pixel alignment and area calculations were

consistent across datasets. Original LULC class values were standardized through a protocolized lookup table, translating each dataset's native classes into three unified categories: Forest, Cropland, and Other. The "Other" land types encompass grassland, urban, barren, wetland, and water. This class reconciliation process was implemented using conditional raster masking, with class assignments explicitly documented in shared code to facilitate reproducibility. To evaluate cross-dataset consistency, pixel-wise difference analysis was performed: for each pixel location, categorical agreement or disagreement was flagged between datasets, generating binary mismatch masks. In cases of pixel-level disagreement, all variants were retained for analysis; disagreement was not resolved by majority rule or exclusion but was instead quantified as part of the overall uncertainty metric. Areas of agreement and disagreement were calculated by tallying the number of matching and non-matching pixels, respectively, for each class. Pixel counts for each class were tallied, and percentage coverage was determined by dividing the class-specific pixel totals by the overall number of pixels. Comparative analysis involved visual and quantitative assessments. For visual comparison, both original and reclassified maps were plotted using a unified color scheme, and side-by-side views facilitated inspection of differences between datasets. Statistical data, including the proportions of Forest, Cropland, and Other, were depicted in bar plots with log-scale axes to accommodate large variations in pixel counts. Quantitative accuracy assessment included constructing confusion matrices for pairwise dataset comparisons. Overall accuracy, representing the proportion of correctly classified pixels, and Cohen's Kappa (κ), which measures inter-dataset agreement beyond random chance, provided overarching agreement metrics. For statistical validation, class-specific accuracy metrics were computed: Forest was evaluated for overestimation and underestimation, Cropland was checked for misclassification against other agricultural or vegetation classes, and Other was examined for potential confusion with built-up areas or water bodies.

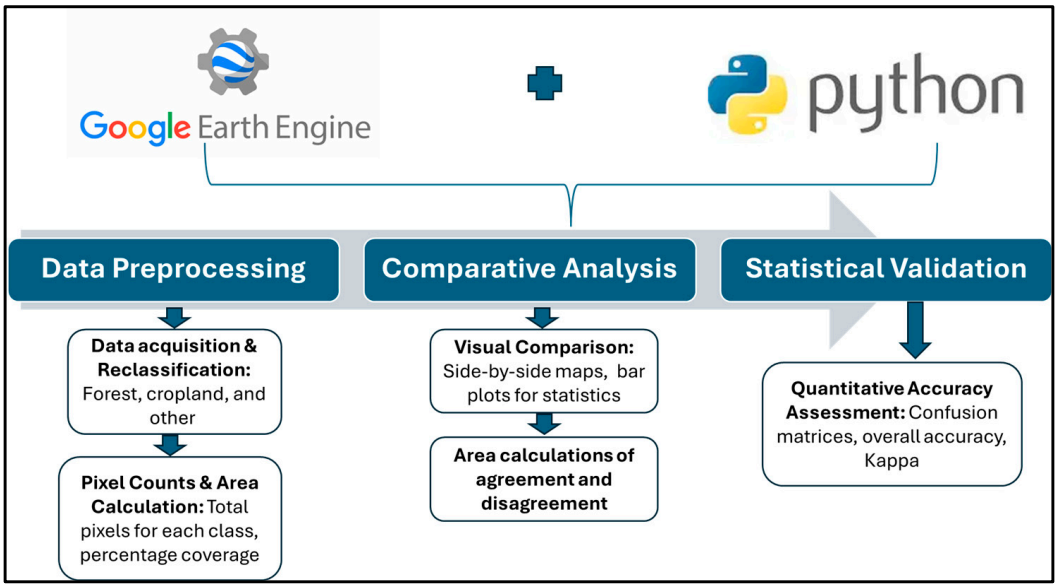


Figure 2. Workflow diagram for historical LULC assessment.

The global future LULC dataset at 1 km resolution produced by Zhang et al. (2023) has been used by many studies to quantify transition patterns between key land cover classes and analyze decadal shifts from 2020 to 2100 [33]. They mapped future land cover changes using the PLUS model, revealing how climate and human activity reshape landscapes with 94% accuracy. For projected LULC changes under different climate and socioeconomic scenarios, the same preprocessing and class reclassification steps were applied to the

global 1 km resolution raster (Figure 3). The SSP projections were not disaggregated to 10 m resolution; instead, they were examined separately at their native scale to avoid introducing spurious precision. For temporal granularity, SSP rasters were evaluated at decadal intervals (2030, 2050, 2070, and 2100).

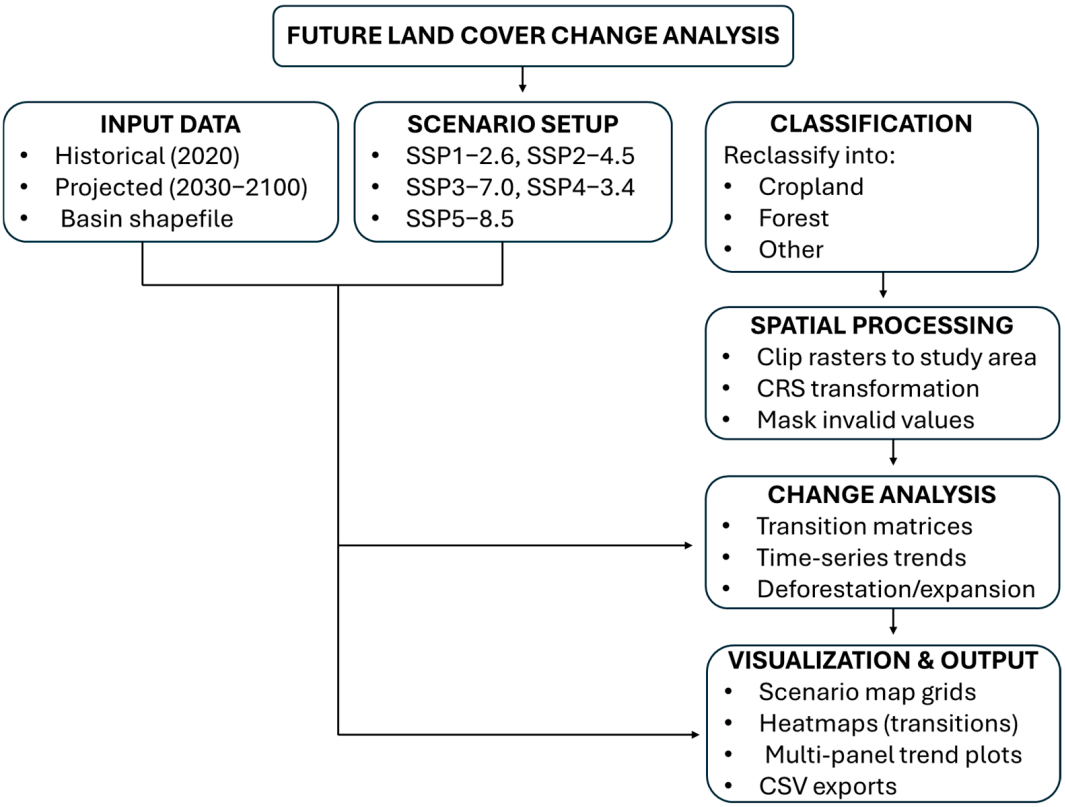


Figure 3. Workflow diagram for future LULC assessment.

The study reclassified land cover into three broad categories (Cropland, Forest, and Other) to simplify cross-scenario comparisons. Using geospatial processing techniques, we clipped and reprojected global 1 km resolution rasters to our study area, ensuring consistent spatial analysis. Transition matrices (Equation (1)) were computed to quantify land cover changes between decadal time steps, while time-series analyses tracked absolute and relative changes in cropland and forest extent. Additionally, we calculated deforestation and cropland expansion rates (Equation (2)) to identify periods of rapid land conversion.

Transition matrices:

$$\boldsymbol{Pij} = \frac{\boldsymbol{Nij}}{\boldsymbol{Ni}} \tag{1}$$

where

Pij = probability of transition from class i to class j,
Nij = number of pixels that changed from class i to class j,
Ni = total number of pixels in class i at the initial time step.

Deforestation and Cropland expansion rates:

$$\boldsymbol{R} = \frac{\boldsymbol{At2} - \boldsymbol{At1}}{\boldsymbol{At1}} \times \mathbf{100} \tag{2}$$

where

R = rate of change (%),
$At1$, $At2$ = area of the land cover class at times $t1$ and $t2$,
$t1$, $t2$ = length of the interval (years).

Results were visualized through a combination of scenario-specific map grids, annotated transition heatmaps, and multi-panel trend plots, facilitating intuitive interpretation of complex land cover dynamics. All analyses were conducted in Python, leveraging geospatial libraries (rioxarray, geopandas) and statistical visualization tools (matplotlib, seaborn) to ensure reproducibility and scalability.

3. Results

3.1. Historical LULC Assessment

3.1.1. Comparison of Land Cover Classifications

Figure 4 presents a comparison of land cover classifications across four global land cover datasets with a focus on Forest, Cropland, and Other land types. It consists of two subplots: land cover percentage by dataset and pixel counts by class (log scale).

In 2017, Figure 4A shows a consistent dominance of the "Other" category across all datasets in the Betsiboka basin. The "Other" class accounts for 92.3% in FROM_GLC10, 93% in ESRI_LULC, and 89.8% in DynamicWorld. This indicates that non-forest and non-cropland areas overwhelmingly dominate the landscape. However, we found substantial variation in forest and cropland estimates between datasets. Forest coverage was reported as only 2.1% in FROM_GLC10, increasing to 3.8% in ESRI_LULC, and reaching the highest value of 7.4% in DynamicWorld. Conversely, Cropland makes up 5.7% in FROM_GLC10 but drops to 3.3% in ESRI_LULC and further to 2.8% in DynamicWorld. These patterns are also reflected in the pixel count distribution, where DynamicWorld shows the highest number of forest pixels (67,476,630) and FROM_GLC10 identifies the most cropland pixels (51,658,839). In 2021, the "Other" category overwhelmingly dominated, comprising 92.6% land cover in ESRI_LULC, 89.4% in DynamicWorld, and slightly less for ESA_LULC, about 88.7%. Forest and Cropland account for a much smaller proportion, with ESA_LULC reporting approximately 4.6% forest and 6.7% cropland, ESRI_LULC showing around 3–4% for both, and DynamicWorld indicating a higher proportion of forest (8.5%) but a lower share of cropland (2.1%). These percentage trends are mirrored in the pixel count panel, where the "Other" category reaches up to 10^9 pixels in all datasets. While ESA_LULC and ESRI_LULC exhibit similar pixel counts for forest and cropland, DynamicWorld records a significantly higher forest pixel count (77,853,034) and the lowest cropland representation (18,970,790) among the three.

The comparison of land cover distributions in the ANP in Figure 4B reveals notable discrepancies in forest and cropland estimates. In 2017, forest cover was 20.6% in FROM_GLC10 to 29.6% in ESRI_LULC and 30% in DynamicWorld, while cropland remained consistently under 3% across all datasets, with DynamicWorld reporting the highest share (2.5%). In 2021, ESA_LULC, ESRI_LULC, and DynamicWorld exhibited slightly higher forest proportions, reaching 34.6%, 30.4% and 32.5%, respectively. However, cropland remained low (<3%) and relatively stable. Pixel count distributions echoed these trends, with forest pixel counts exceeding 10^7 in ESRI_LULC and DynamicWorld, whereas cropland pixel counts remained below 10^6. The discrepancies observed among datasets, particularly for cropland, can be attributed to several factors such as class imbalance, spectral confusion and methodological differences across datasets. The "Other" land cover class remained dominant across all datasets and years, accounting for over 60% of total area. These differences highlight the sensitivity of land cover classification to dataset selection.

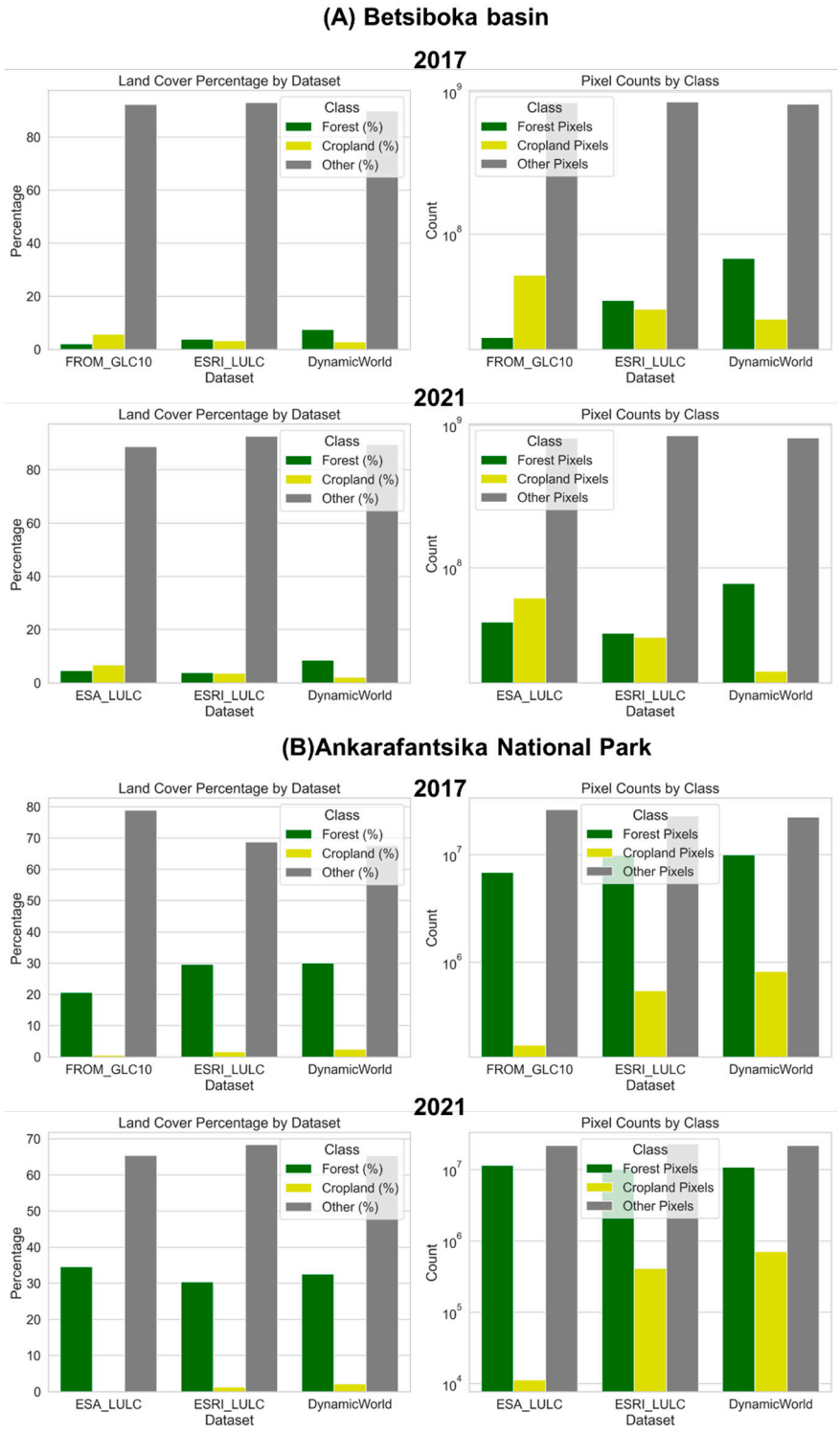


Figure 4. Land cover statistics across the Betsiboka basin (**A**) and ANP (**B**) between 2017 and 2021. Land cover classes: Forest (green), cropland (yellow), and other (gray). Percentage of land use type per dataset (**left panel**) and pixel count by class (**right panel**).

3.1.2. Accuracy Assessment of Land Use Datasets

The tables below illustrate a comparative accuracy metric of four high-resolution global LULC datasets. The assessment is based on pixel-level agreement with reference data using standard evaluation metrics: Overall Accuracy (OA), Kappa coefficient, User's Accuracy (UA), and Producer's Accuracy (PA). OA measures the proportion of correctly classified instances, while Kappa adjusts for agreement that could occur by chance. A series

of confusion matrices comparing the agreement between these datasets was provided in Appendix A, Figure A1.

As shown in Table 2, the inter-comparison of LULC datasets in Betsiboka revealed significant variations in classification agreement between 2017 and 2021. While overall accuracy (OA) remained consistently high (88–92%), the Kappa coefficients (0.31–0.52) indicated only fair to moderate agreement beyond chance. These results suggest substantial class imbalance, likely due to dominant "Other" land cover. The ESRI_LULC vs. DynamicWorld comparison demonstrated the highest consistency in both years (OA = 92%, Kappa = 0.51–0.52), particularly for non-vegetated classes (UA = 97–98%). However, forest classification exhibited persistent overestimation (PA = 93–95% vs. UA = 43–47%), while cropland detection remained problematic (PA $\leq$ 35%, UA $\leq$ 53%). The 2021 results showed minimal improvement from 2017, with ESA-based comparisons performing similarly (Kappa = 0.44). These findings highlight two critical challenges: (1) the need for balanced accuracy assessments that account for class distribution, and (2) fundamental limitations in distinguishing cropland and fragmented forest areas across all products. The consistently low cropland PA (<35%) suggests either definitional inconsistencies between datasets or spectral confusion in this agricultural region. It is important to note that Cropland remains fundamentally unreliable across datasets and that findings on cropland change should be interpreted with caution. The integration of higher-resolution temporal data and ancillary datasets can improve classification.

Table 2. Comparative performance of LULC datasets in the Betsiboka basin.

2017								
Comparison	**OA**	**Kappa**	**Forest_PA**	**Forest_UA**	**Cropland_PA**	**Cropland_UA**	**Other_PA**	**Other_UA**
FROM_GLC10 vs. ESRI_LULC	0.91	0.33	0.76	0.42	0.16	0.29	0.96	0.95
FROM_GLC10 vs. Dynamic-World	0.88	0.31	0.95	0.27	0.11	0.22	0.93	0.96
ESRI_LULC vs. Dynamic-World	0.92	0.52	0.93	0.47	0.35	0.41	0.94	0.98
2021								
Comparison	**OA**	**Kappa**	**Forest_PA**	**Forest_UA**	**Cropland_PA**	**Cropland_UA**	**Other_PA**	**Other_UA**
ESA_LULC vs. ESRI_LULC	0.90	0.44	0.61	0.73	0.24	0.45	0.97	0.93
ESA_LULC vs. Dynamic-World	0.89	0.44	0.87	0.46	0.15	0.47	0.94	0.94
ESRI_LULC vs. Dynamic-World	0.92	0.51	0.95	0.43	0.31	0.53	0.94	0.97

OA = Overall Accuracy; PA = Producer's Accuracy; UA = User's Accuracy.

Table 3 shows notable variations in classification consistency in ANP between 2017 and 2021. In 2017, ESRI_LULC and DynamicWorld exhibited the strongest agreement (OA = 94%, Kappa = 0.86), with high producer's (PA) and user's (UA) accuracies for forest (PA = 94%, UA = 93%) and "Other" land cover (PA = 95%, UA = 96%). However, cropland classification remained problematic across all comparisons (PA = 10%, UA = 2% for

FROM_GLC10), indicating significant misclassification or underestimation. By 2021, overall agreement improved, with ESRI_LULC vs. DynamicWorld achieving near-perfect consistency (OA = 95%, Kappa = 0.90), particularly for forest (PA = 99%, UA = 92%) and "Other" classes (PA = 94%, UA = 99%). Despite this progress, cropland accuracy remained low (PA = 27–63%, UA = 1–37%), suggesting persistent challenges in distinguishing cropland from other categories. These results highlight the reliability of ESRI_LULC and DynamicWorld for forest and non-cropland mapping but underscore the need for refined cropland classification methods in heterogeneous landscapes like Ankarafantsika.

Table 3. Comparative performance of LULC datasets in the ANP.

2017								
Comparison	**OA**	**Kappa**	**Forest_PA**	**Forest_UA**	**Cropland_PA**	**Cropland_UA**	**Other_PA**	**Other_UA**
FROM_GLC10 vs. ESRI_LULC	0.88	0.70	0.98	0.68	0.07	0.02	0.86	0.99
FROM_GLC10 vs. DynamicWorld	0.87	0.68	0.98	0.67	0.10	0.02	0.85	0.99
ESRI_LULC vs. DynamicWorld	0.94	0.86	0.94	0.93	0.60	0.40	0.95	0.96
2021								
Comparison	**OA**	**Kappa**	**Forest_PA**	**Forest_UA**	**Cropland_PA**	**Cropland_UA**	**Other_PA**	**Other_UA**
ESA_LULC vs. ESRI_LULC	0.94	0.87	0.87	0.99	0.37	0.01	0.98	0.93
ESA_LULC vs. DynamicWorld	0.95	0.89	0.93	0.99	0.27	0.00	0.96	0.96
ESRI_LULC vs. DynamicWorld	0.95	0.90	0.99	0.92	0.63	0.37	0.94	0.99

OA = Overall Accuracy; PA = Producer's Accuracy; UA = User's Accuracy.

Figure 5 represents the class-specific accuracy metrics among all datasets. The three land cover classes analyzed are Forest, Cropland, and Other, with three pairwise dataset comparisons per year. The *y*-axis represents accuracy values ranging from 0 to 1, and error bars denote variability (confidence interval).

Figure 5 depicts distinct patterns of agreement between the Betsiboka basin and ANP, highlighting region-specific classification challenges. Forest classification performed better in Ankarafantsika (high accuracy > 0.8) than in Betsiboka (accuracy > 0.6) in all datasets for both years. These findings highlight the predominance of forested areas within the park, despite ongoing increases in fire incidents and deforestation. Cropland remained the most challenging class to classify accurately in both regions. This might likely be due to seasonal variability, crop heterogeneity, and confusion with other vegetative classes. The "Other" class maintained very high accuracy (>0.90) in both regions, indicating strong inter-dataset agreement. Comparatively, the overall trend from 2017 to 2021 reflected marginal gains in classification accuracy, particularly for forest and cropland classes. These improvements might be attributed to advancements in satellite sensor resolution, refined classification algorithms, and improved dataset harmonization. Overall, the ESRI_LULC vs.

DynamicWorld pairing emerged as the most reliable in both regions, though its performance was markedly stronger in ANP.

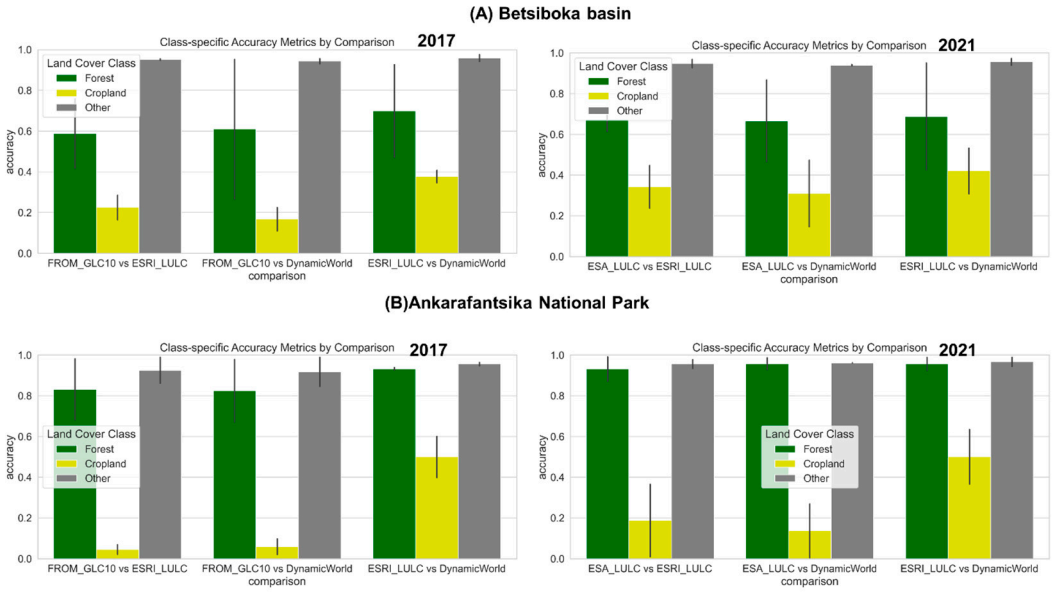


Figure 5. Comparison of land use type accuracy metrics in the Betsiboka basin and ANP.

3.1.3. Comparison of the Spatial Representation of Forest and Cropland

The reclassified land cover maps for 2017 and 2021 reveal notable spatial differences across datasets (Figure 6).

In the Betsiboka basin (A), Dynamic World consistently delineates dense and continuous forest cover, particularly downstream. In contrast, FROM_GLC10 underrepresents forest cover, while ESRI_LULC and ESA_LULC depict moderate to extensive coverage, though with varying degrees of fragmentation. For cropland, ESA_LULC and ESRI_LULC show broader spatial extent, especially in 2021, suggesting expansion. Dynamic World mapped contiguous patches of forest, while FROM_GLC10's forest class appeared highly fragmented in the study area. The "Other" category is dominant across datasets, especially in FROM_GLC10, likely due to misclassification. Forest cover remains relatively stable, but with minor fragmentation. Although no major deforestation is evident, slight forest fragmentation may indicate emerging degradation. Cropland expansion is notable in ESA_LULC and ESRI_LULC. These findings underscore how dataset choice shapes land cover interpretation, with Dynamic World and ESRI_LULC providing more reliable forest and cropland estimates, respectively. Accurate spatial data are essential for land use modeling, carbon assessments, and conservation planning.

In ANP (B), forest cover is the dominant land class and extensive in the upstream areas across all datasets, though its spatial extent varies. In contrast, the downstream exhibits notable changes, with increasing cropland expansion and forest fragmentation from 2017 to 2021, particularly evident in the Dynamic World and ESRI_LULC datasets. While ESA_LULC presents a more conservative view of land cover change, the other datasets suggest intensified agricultural activity and possible deforestation in the lower basin. For instance, ESRI_LULC shows stable cropland areas, with a slight 2021 increase possibly due to agricultural expansion. DynamicWorld maps cropland more conservatively but with coherent spatial clustering. FROM_GLC10 underrepresents cropland, while ESA_LULC shows minimal coverage, likely due to misclassification. The "Other" class is widespread, especially in FROM_GLC10, indicating potential misclassification or coarse resolution. Overall, DynamicWorld provides the most precise forest delineation, while

ESRI_LULC better identifies cropland. These observed patterns highlight growing land use pressures downstream and the need for targeted conservation and land management efforts to mitigate environmental degradation in the basin.

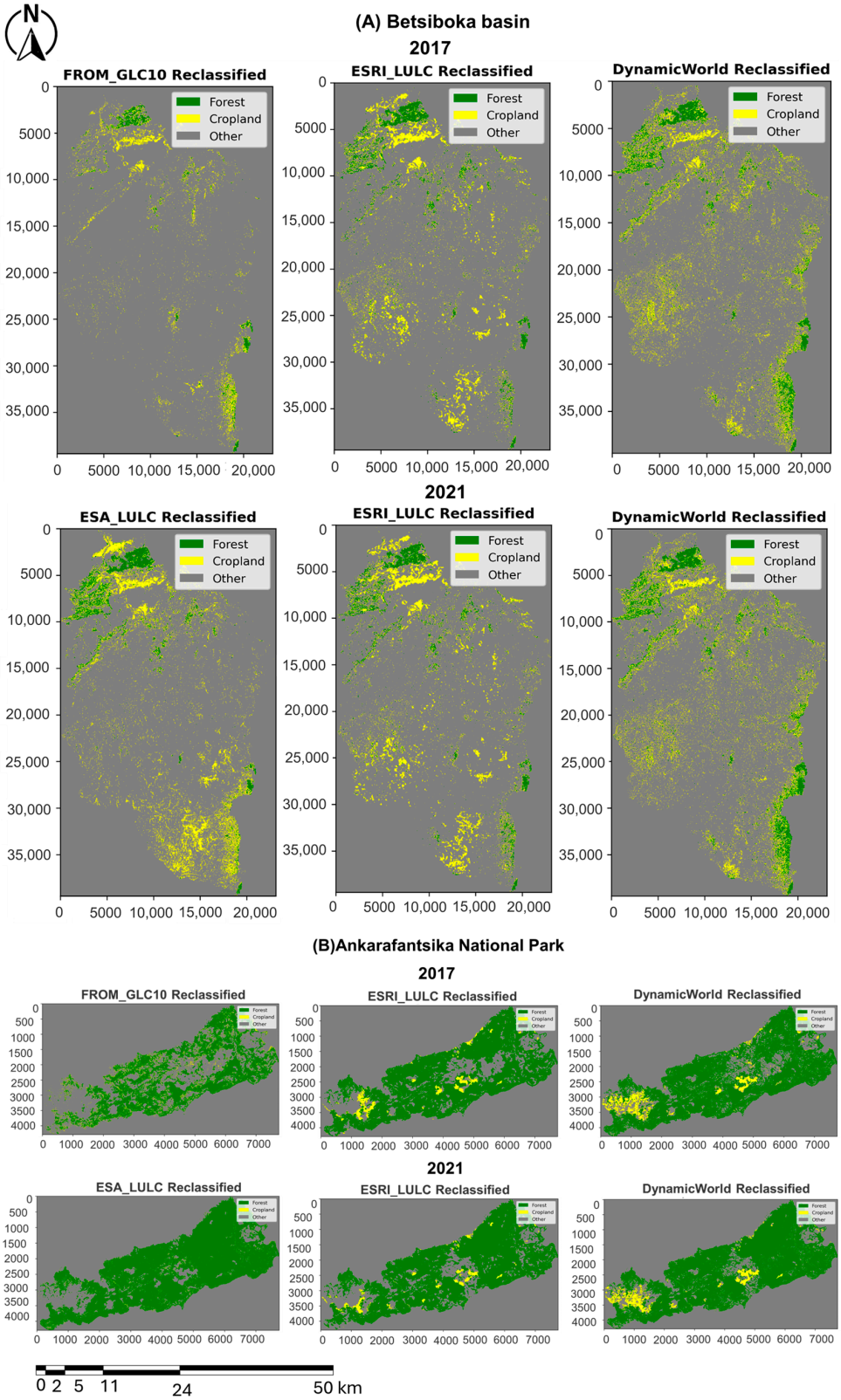


Figure 6. Spatial patterns of reclassified land cover map (Forest: Green, Cropland: Yellow, and Other: Gray) across the Betsiboka basin and ANP from 2017 to 2021.

3.2. Future LULCC Analysis

3.2.1. Systematic Comparison of Land Cover Change Across Climate Scenarios

Exploring future land use trajectories in northwestern Madagascar reveals striking contrasts between two landscapes Betsiboka basin and the ANP. Figure 7 presents projections under five SSPs, highlighting both absolute land area (km^2) and relative percentage change from 2020 to 2100. In the Betsiboka basin (A), all scenarios predict substantial forest expansion over the 21st century. Under SSP5, forest area grows from approximately 10,500 km^2 in 2020 to over 42,000 km^2 by 2100, a remarkable 300% increase. SSP3 and SSP2 also show strong upward trends, with forest cover exceeding 35,000 km^2, representing growth of over 230% and 200%, respectively. Even SSP1, which prioritizes sustainability, projects a more modest but still significant increase to 25,000 km^2, a 140% rise compared to 2020. Cropland remains relatively stable in absolute terms but shows notable variation across scenarios. Under SSP4 and SSP5, nearly doubles from around 5000 km^2 in 2020 to approximately 10,000 km^2 by 2100 (+100%). In contrast, SSP1 shows a decline to about 3500 km^2, reflecting a shift toward forest restoration or alternative land uses. Meanwhile, 'Other' land types decline across most scenarios, falling from over 35,000 km^2 in 2020 to below 15,000 km^2 by 2100, a 60% reduction, indicating a potential large-scale reforestation or land use conversion effort. The decline likely reflects reclassifications and transitions into forest or cropland categories in the model rather than actual ecosystem transformations.

In ANP (B), land cover remains more stable in both absolute and relative terms, though not without surprises. Under SSP2, SSP3, SSP4, and SSP5, forest area remains nearly unchanged, holding at 900 km^2 from 2020 to 2100 (0–5% change). However, SSP1 deviates sharply from its sustainability narrative. Between 2070 and 2100, forest cover drops from 900 km^2 to just 400 km^2, representing a 55% decrease from 2020 levels. Simultaneously, 'Other' land within the park increases to nearly 700 km^2, suggesting possible degradation or land conversion pressures. Cropland remains minimal across all SSPs, staying well below 100 km^2, with slight increases under SSP1 and SSP5 by 2070. This likely reflects model assumptions, coarse resolution, and aggregation effects, underscoring that significant local-scale changes may still occur and should be considered in the context of food security. This stability emphasizes the park's role as a conserved area but also reveals its limits under certain development scenarios.

By mid-century, the trends became more distinct. In the Betsiboka basin, forest area rises to over 32,000 km^2 by 2050 and surpasses 37,000 km^2 by 2070, aligning with consistent percentage gains of 200–250% from the baseline. Meanwhile, cropland stays within 4000–5000 km^2, and 'Other' land continues to contract. These shifts reflect either ambitious reforestation efforts or land management transformations that prioritize forest recovery. ANP, by contrast, remains largely unchanged through 2070 forest cover holding steady at 950–1000 km^2, reinforcing its perceived ecological stability. Yet, the sudden 55% forest loss under SSP1 by 2100 introduces concerns about the resilience of protected areas under evolving socioeconomic pressures. This finding aligns with the projections made by Rafanoharana et al. (2024) [24]. They estimated a reduction of 25% (9306 km^2) in the overall area of protected forests in Madagascar from 2017 to 2050, under the assumption of stable deforestation rates.

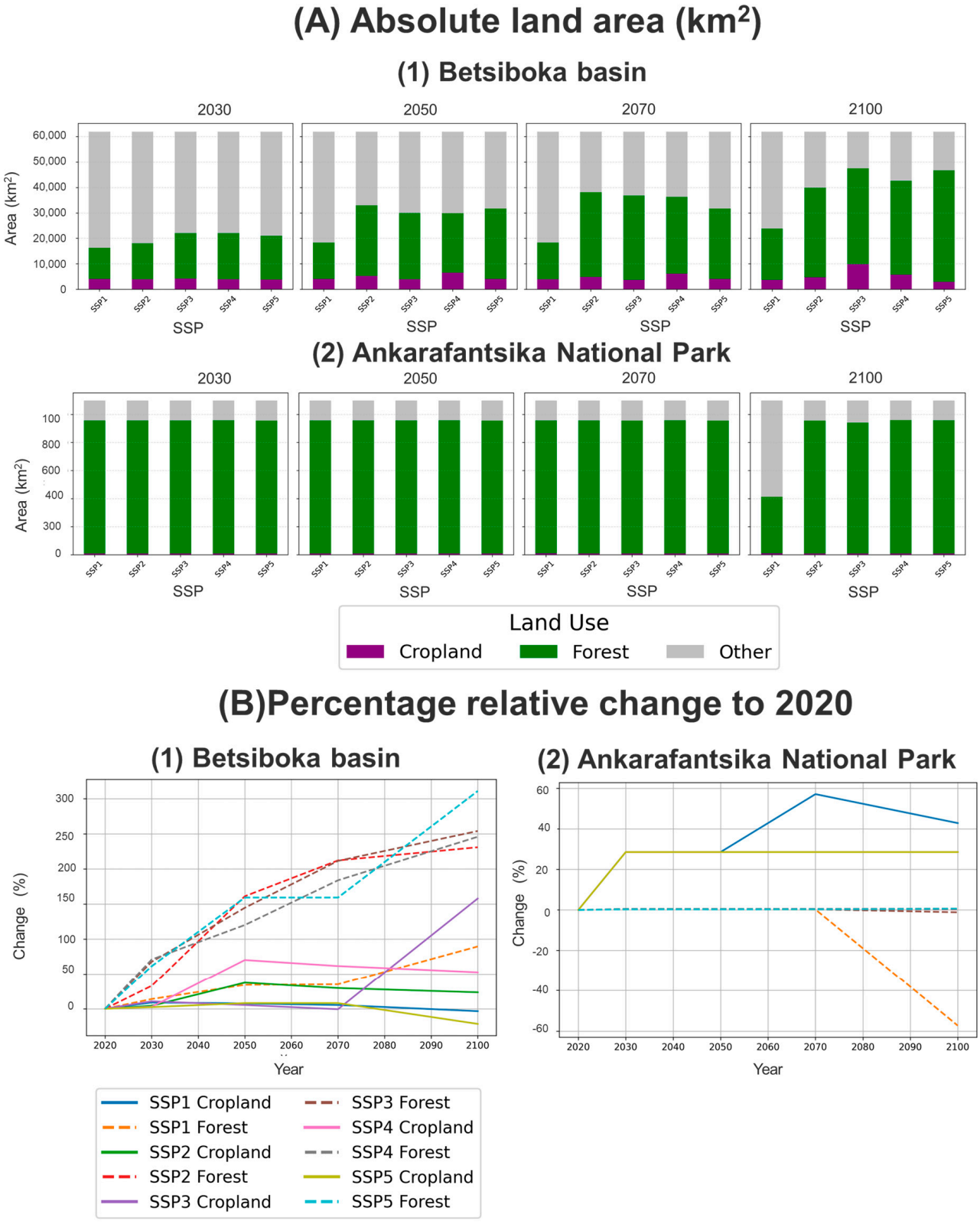


Figure 7. Comparison of projected LULCC across five SSPs (SSP1 to SSP5) for the Betsiboka basin (**1**) and Ankarafantsika National Park (**2**) across four time horizons (2030, 2050, 2070, and 2100). (**A**) Absolute land area in km^2 and (**B**) Percentage relative change to 2020 in %. Three land use categories: cropland (purple), forest (green), and other land (gray).

3.2.2. Spatiotemporal Dynamics of Projected LULC

Figure 8 reveals distinct spatial and temporal patterns in cropland, forest, and other land categories in the Betsiboka basin. Across all scenarios, a general trend of forest expansion and decline in "Other" land types is observed from 2030 to 2100, though the extent and timing of these changes vary considerably. Notably, SSP1–RCP2.6 and SSP5–RCP8.5 show the strongest gains in forest cover, particularly in the upstream and midstream of the basin. This suggests either successful sustainable land management (SSP1) or large-scale biome shifts under intensive development (SSP5). In contrast, SSP3–RCP7.0 exhibits limited forest recovery and continued cropland expansion, especially in the downstream region. These changes might reflect weak environmental governance and high land use pressure. Temporal comparisons indicate that cropland expansion typically peaks by 2050 under most scenarios, followed by stabilization or decline. SSP3 was an exception, where cropland continues to grow into 2100. Spatially, the downstream region remains the core agricultural zone across all scenarios, while the upstream area emerges as a key frontier for either forest regeneration or degradation, depending on the development pathway. Rakotoarimanana et al. (2024) also predicted an expansion of the agricultural land in the downstream areas of the Betsiboka basin by 2050 [29]. These findings highlight the importance of both policy direction and spatial context in shaping future land use trajectories in the basin.

Regarding the case of ANP (Figure 9), Forest cover remains largely intact throughout the projection period under the sustainability-focused SSP1–RCP2.6 scenario. By 2100, only minor expansions of cropland and other land types are observed, suggesting strong forest persistence under low emissions and pro-environmental development pathways. In contrast, SSP2–RCP4.5 shows moderate forest loss over time, particularly in the southern and western edges of the park. While forests remain dominant, there is a gradual increase in cropland and other land use categories by 2100. SSP3–RCP7.0 and SSP5–RCP8.5 (higher emissions and weaker environmental governance) demonstrate a more pronounced land cover change. There was a visible expansion of cropland and other land types across the park landscape by the end of the century. This suggests declining forest integrity under conditions of rapid population growth and limited regulation. SSP4–RCP3.4 (high inequality and regionally fragmented governance) shows an intermediate pattern. Although forest remains dominant, there is observable conversion to cropland and other land uses after 2070, primarily in areas adjacent to existing settlements. This scenario highlights the vulnerability of forest systems under socioeconomic disparity, even when emissions are not at the highest levels. Overall, the spatial patterns reveal that the forest cover in the ANP was highly sensitive to both emission trajectories and socioeconomic assumptions. Scenarios with lower emissions and strong environmental management (SSP1–RCP2.6) are associated with minimal forest loss, whereas high-emission, development-intensive pathways (SSP5–RCP8.5) lead to significant land conversion. A prior study warned that without action on climate change, Madagascar's forests could suffer drastic damage by 2080. These findings underscore the importance of integrated conservation strategies to buffer protected areas from future land use pressures.

In summary, the synthesized patterns across the Betsiboka basin and ANP revealed contrasting LULC dynamics. Forest recovery in Betsiboka hinges on converting "Other" land into forest rather than reducing cropland, whereas the resilience of ANP's forests depends on sustained environmental management. These findings highlight the necessity of integrated and adaptive conservation strategies to mitigate land use pressures and climate change impacts.

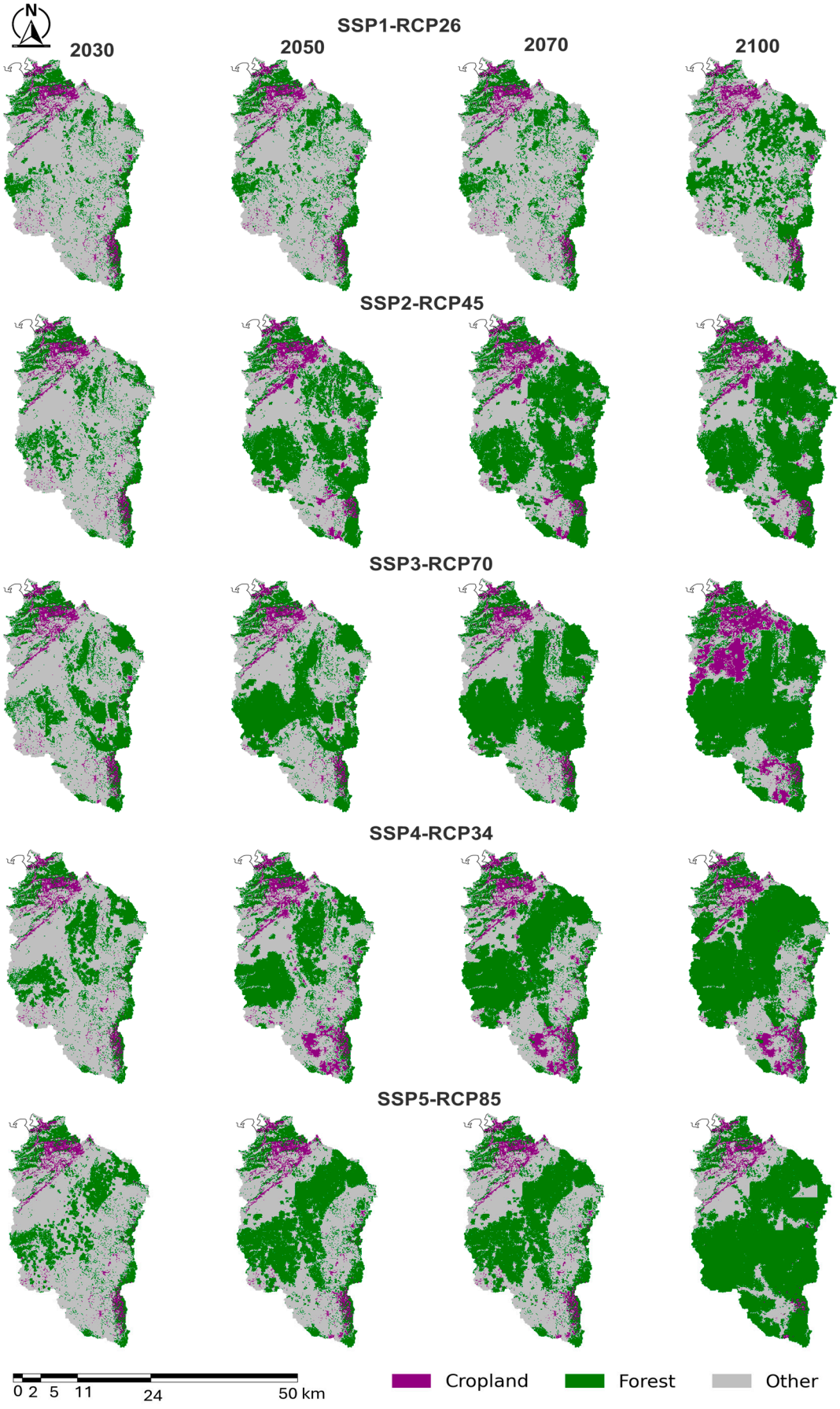


Figure 8. Spatial distribution of projected LULC in the Betsiboka Basin under 5SSPs (SSP1–SSP5) for 2020 to 2100.

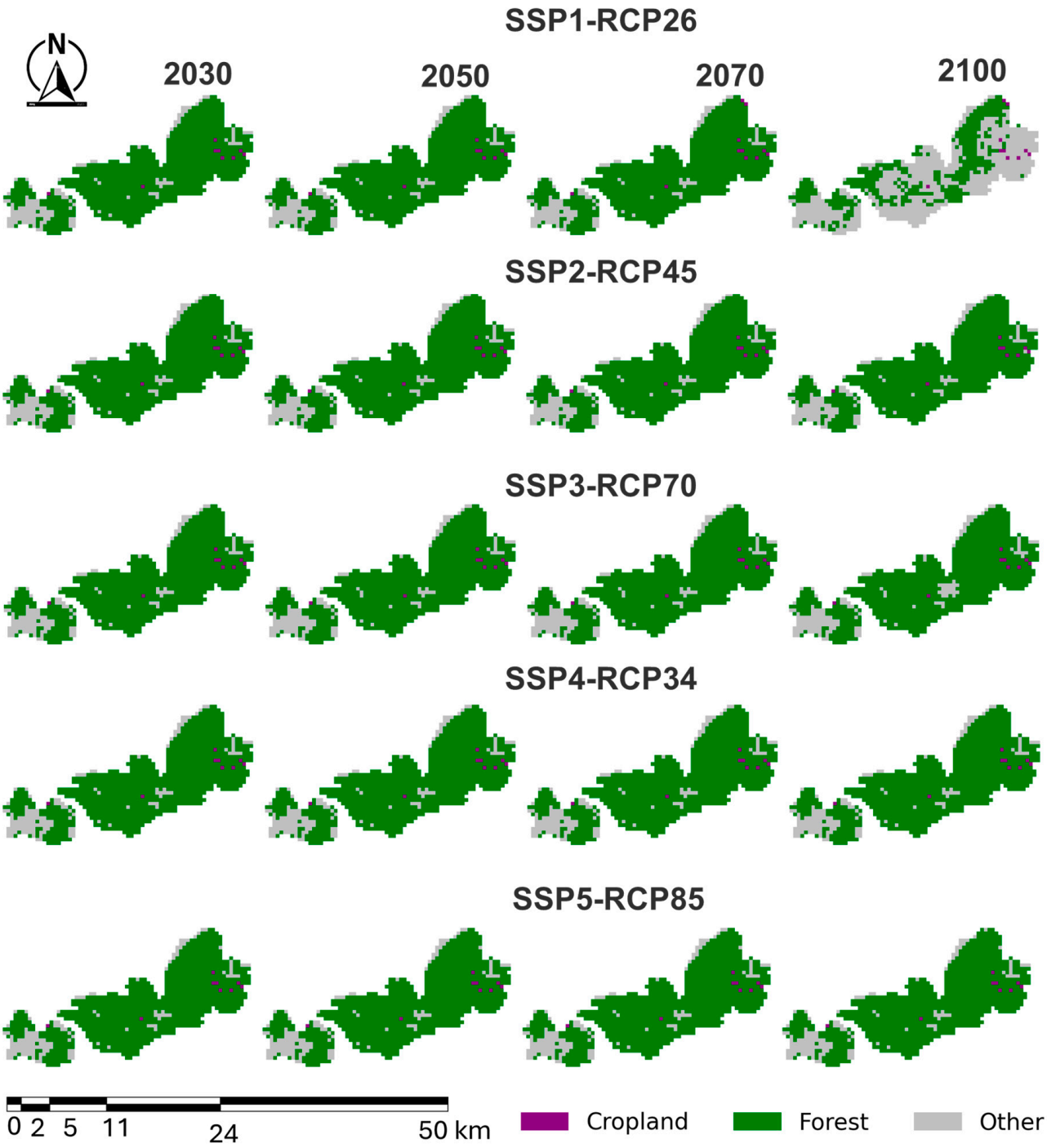


Figure 9. Spatial distribution of projected LULC in the Ankarafantsika National Park under 5SSPs (SSP1–SSP5) for 2030 to 2100.

3.2.3. Quantification of Transition Patterns Between Land Cover Types

Figure 10 displays land cover transition matrices for the Betsiboka basin under five SSP–RCP scenarios, showing temporal changes across four intervals: 2020–2030, 2030–2050, 2050–2070, and 2070–2100. Results highlight substantial forest expansion across all scenarios, while cropland areas remain relatively stable, and "Other" land cover decreases significantly. Under SSP1–RCP2.6, forest area increased from 41,759 km^2 (100.0% of the original forest area) in 2030 to 43,598 km^2 in 2050, 43,598 km^2 in 2070, and ultimately reached 45,643 km^2 by 2100, an increase of approximately 3884 km^2 compared to 2030. Most of this gain came from the transition of "Other" land cover into forest, which de-

creased from 6543 km^2 in 2030 to 2851 km^2 by 2100. Cropland area remained largely constant, ranging from 1707 km^2 in 2030 to 1967 km^2 in 2070, then slightly declining to 735 km^2 by 2100. In SSP2–RCP4.5, forest expansion was more rapid. Forest area rose from 14,071 km^2 in 2030 to 22,793 km^2 in 2070 and reached 31,164 km^2 by 2100. These gains were predominantly sourced from the reduction in "Other" land cover, which declined from 28,899 km^2 in 2030 to 21,964 km^2 in 2100. Cropland area increased slightly over the century, from 1733 km^2 in 2030 to 4756 km^2 in 2100. Under SSP3–RCP7.0, the largest forest expansion was observed. Forest cover grew from 17,255 km^2 in 2030 to 25,961 km^2 in 2070 and reached 32,871 km^2 by 2100, representing an overall increase of 15,616 km^2 between 2030 and 2100. This growth corresponded to a steady decline in "Other" land, which dropped from 31,831 km^2 in 2030 to 14,314 km^2 in 2100. Cropland area showed minimal change, remaining around 1683–1347 km^2 across the century. SSP4–RCP3.4 projected forest increases from 18,151 km^2 in 2030 to 23,357 km^2 in 2070, eventually reaching 30,183 km^2 by 2100—an increase of 12,032 km^2 since 2030. The area of "Other" land decreased from 30,964 km^2 in 2030 to 13,518 km^2 in 2100. Cropland remained low, starting at 1648 km^2 in 2030 and fluctuating slightly to 1004 km^2 in 2100. Lastly, under SSP5–RCP8.5, forest area expanded from 17,317 km^2 in 2030 to 27,356 km^2 in 2070 and reached 33,514 km^2 by 2100. The decline in "Other" land was again substantial, decreasing from 30,162 km^2 in 2030 to just 13,308 km^2 in 2100. Cropland increased marginally, from 1640 km^2 in 2030 to 3414 km^2 in 2100. Across all SSP–RCP combinations, the dominant pattern was a large-scale conversion of "Other" land cover into forest. By 2100, over 70% of "Other" lands in 2020 had transitioned into forest in all scenarios except SSP1–RCP2.6, where forest gains were more moderate. Cropland showed minor increases, suggesting that forest expansion will not occur at the expense of agricultural land. Previous studies reported that forest and grassland conversion to agriculture and urban areas endangered Madagascar's biodiversity, along with food and water security [34,35]. Species in western and southern Madagascar face the greatest forward velocities, and the distances needed to keep pace with the shifting climate [36].

Overall, the results reveal that the Betsiboka basin is projected to experience widespread forest recovery through the 21st century. The extent and rate of this transition vary by scenario, with the highest gains in forest cover occurring under SSP3–RCP7.0 and SSP5–RCP8.5.

Figure 11 illustrates the land cover transitions in the ANP under five SSPs. Across all SSPs scenarios, forest cover in ANP remains the dominant land cover type from 2030 to 2070, consistently occupying approximately 942–949 km^2 (99.7–100%). No significant expansion of cropland is observed under any scenario, except for isolated instances of 1–2 km^2 transitions under SSP3–RCP70 and SSP5–RCP85. Notably, transitions from forest to "Other" land cover types begin to emerge by 2100 under certain scenarios. The most substantial change occurred under SSP1–RCP26, where forest area declined to 584 km^2 (a 39.4% reduction). Despite the low emissions, these results suggest potential degradation or reclassification to non-productive land. SSP5–RCP85 and SSP3–RCP70 also display forest loss of 2.2% and 1.4%, respectively, while SSP2–RCP45 and SSP4–RCP34 maintain nearly complete forest cover (100%) across all time steps. In summary, while the park's forest is largely resilient in the near term, long-term projections reveal vulnerability even under sustainable pathways. These patterns highlight the importance of sustained and adaptive forest management strategies beyond mid-century.



Figure 10. Land cover transitions under future scenarios in the Betsiboka basin under five SSPs (SSP1–SSP5) across four future time horizons: 2020–2030, 2030–2060, and 2060–2080.

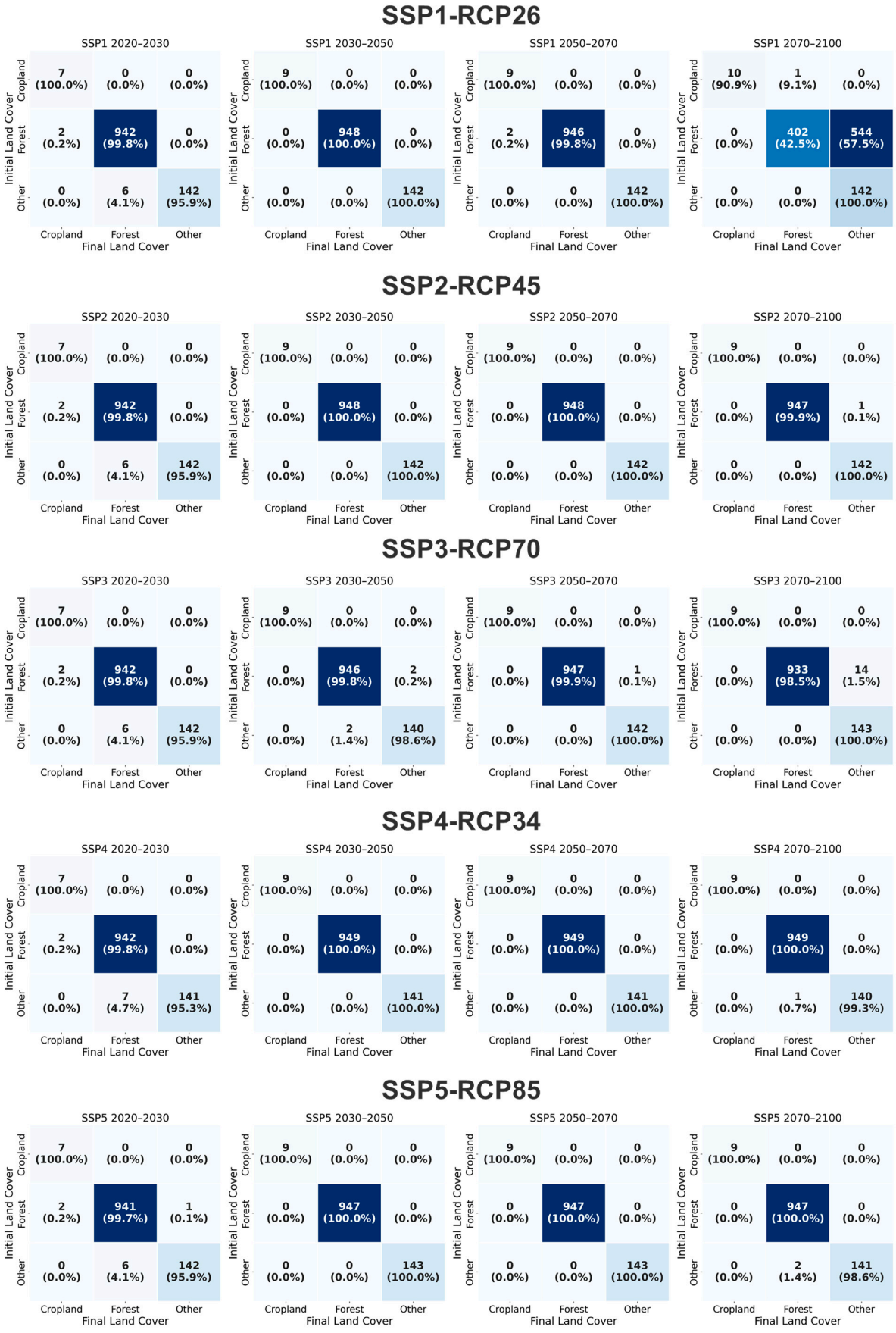


Figure 11. Projected land cover transitions within ANP under five SSPs (SSP1–SSP5) across four future time horizons: 2020–2030, 2030–2060, and 2060–2080.

4. Discussion

In addressing the first research question, our discussion highlights the spatial concordance and divergence among various LULC datasets. Across all datasets and years, "Other" land cover dominated both the Betsiboka basin and ANP, while forest and cropland occupied smaller, highly variable proportions. This underscores that forest and cropland estimates differ significantly by dataset, especially in the ANP, where DynamicWorld and ESRI_LULC yield more consistent results. Another important finding was that ANP demonstrated significantly stronger inter-dataset agreement (Kappa = 0.68–0.90) than Betsiboka basin (Kappa = 0.31–0.52). Both regions achieved high overall accuracy (OA > 88%). This indicates that LULC products were more consistent in ANP compared to Betsiboka. This discrepancy likely reflects ANP's more homogeneous vegetation cover and conservation-oriented land management, which support greater classification consistency. By contrast, Betsiboka's fragmented agricultural mosaic and seasonal crop cycles increase classification uncertainty, underscoring the influence of landscape heterogeneity, management practices, and seasonality on LULC product comparability. This study has demonstrated that forest classification was more accurate in the ANP (UA 67–98%) than in Betsiboka (UA = 27–73%). Cropland detection was poor, especially in Betsiboka (PA $\leq$ 35% vs. $\leq$64% in ANP). The "Other" class had high accuracy (UA > 93%) in both regions. Comparing these results with other studies, the land cover map accuracy ranges from 73.4% to 83.8% at the global level, with ESA WorldCover performing best, followed by Dynamic World and ESRI LULC [10]. In contrast, Venter et al. (2022) reported that ESRI achieved the highest overall accuracy at 75%, outperforming both Dynamic World and ESA WorldCover, which each had an accuracy of 65% [9]. In Southeast Asia, ESA2020 had the highest accuracy (81.1%), followed by ESRI2020 and FROM_GLC10 [37]. While cropland, forest, and built-up areas were mapped well, classes like shrubland, wetland, and bare land showed lower accuracy. For improved accuracy, they recommended combining different datasets: FROM_GLC10 for cropland and water, ESRI2020 for shrubland and built-up areas, and ESA2020 for forest, grassland, wetland, and bare land. Mudele et al. (2025) observed strong spatiotemporal agreement among FROM-GLC, ESRI, MFGFC, PALSAR, and ESA in Madagascar, validating their use for robustness checks [14]. However, Dynamic World showed the lowest correlation with other products for both forest and deforested regions. Moreover, this study sought to determine the most suitable datasets for monitoring the forest and cropland in the Betsiboka basin and ANP. We found that FROM-GLC10 and ESA WorldCover provided more reliable cropland estimates, while Dynamic World and ESRI Land Cover were better for assessing forest areas in the Betsiboka Basin. DynamicWorld and ESRI_LULC offer more consistent estimates of forest and cropland cover in the ANP. These results underscore the importance of class-specific accuracy evaluation in LULC analysis. While broad land cover categories such as "Other" show high consistency among datasets, cropland detection requires further methodological development to improve their reliability for applications such as land use modeling and land change detection. These results therefore need to be interpreted with caution. The LULC projections reveal two divergent futures. Surprisingly, aggressive forest expansion up to +300% are expected to occur in the Betsiboka basin under SSP3 and SSP5 scenarios transforming the landscape dramatically. In contrast, ANP appears stable but not immune to future threats, particularly under SSP1. Several possible factors may contribute to these outcomes, including model assumptions (PLUS-based reforestation trends), scale limitations (1 km resolution cannot capture smallholder deforestation), and other sources of uncertainty. These outputs should be interpreted as model-driven scenarios with considerable uncertainty, rather than ecological forecasts, especially given Madagascar's ongoing deforestation pressures. The contrast between scenarios and periods illustrates how policy

decisions and socioeconomic developments can drive dramatic differences in both absolute land area and percentage change, even within the same geographic region.

In Madagascar, the ecological and socioeconomic implications of land use change are particularly pronounced. Forest recovery in some regions can contribute to biodiversity conservation in one of the world's most species-rich and threatened [22], while also enhancing ecosystem services such as watershed protection and carbon storage [21]. Reforestation and strict conservation measures may reduce the availability of arable land for smallholder farmers [38]. However, stable cropland trends at the national scale may hide local issues like shifting cultivation, land encroachment, and declining soil fertility, all of which threaten food security [39]. These dynamics show the balance needed between conservation and agriculture, emphasizing integrated land management for both biodiversity and local livelihoods.

This study significantly advances the understanding of present and future LULC in a biodiversity hotspot in northwestern Madagascar. Here are the recommendations identified for improving future research based on the findings of this study:

- In the Betsiboka basin, FROM-GLC10 and ESA WorldCover provided more reliable cropland estimates, while Dynamic World and ESRI Land Cover were better for assessing forest areas. In the ANP, Dynamic World, and ESRI Land Cover offer more consistent estimates of forest and cropland cover. A limitation is the temporal mismatch among LULC datasets (2017–2023), though aligning them to the 2017–2021 period helped minimize bias. We recommend careful consideration of dataset characteristics when applying these products in Madagascar. Future work could incorporate ground truth data for validation and expand the comparison to additional datasets.
- The future projections revealed two divergent futures. Aggressive forest expansion will transform the landscape in Betsiboka dramatically. In contrast, ANP land cover appears stable but not immune to future threats. The uncertainty and accuracy of the future LULC data used in our analysis were a limitation, despite its high resolution [40]. Uncertainties in future LULC datasets arise from multiple sources, including the translation of SSP narratives into quantitative land use pathways, spatial downscaling methods, and assumptions within the models. For Madagascar, important local drivers such as shifting cultivation (tavy), traditional land tenure, governance, protected area enforcement, and national policies are indirectly represented in global frameworks. Nevertheless, these factors greatly affect outcomes like cropland expansion, deforestation, and land degradation. Future studies should compare these data with other future LULC datasets that use ground data for scenario-based land use projections.
- Cropland remained broadly stable, though scenario-specific expansions suggest that forest expansion will not occur at the expense of agricultural land. The aggregation of land cover into Forest, Cropland, and Other, while analytically convenient, is a limitation as it may obscure finer-scale dynamics and transitions relevant to landscape change. To address food insecurity, agricultural intensification is suggested to increase food production on existing croplands. This can be complemented by integrating agroforestry practices [41] to leverage forests as a source of diverse foods and income.

5. Conclusions

This study aimed to assess the historical and future changes in forest and cropland in the Betsiboka basin and the ANP. We compared five high-resolution global land cover datasets (2017–2100) using GEE and Python. Despite extensive research on deforestation in Madagascar, the dynamics of cropland expansion remain poorly understood. Previous study found that global change will lead to poverty and food insecurity in Madagascar [42].

Famine and drought were reported as the leading factors driving internal migration in Madagascar [43]. Addressing the research questions, the results indicate that forest and cropland areas in the Betsiboka basin varied widely across datasets. Results showed that "Other" land dominated, with forest and cropland remaining minimal across datasets. While forest classification proved more reliable in ANP than in Betsiboka, cropland detection, particularly in Betsiboka, remains a significant challenge due to low producer accuracy. The high accuracy of the "Other" class across both regions suggests that certain land cover transitions are well captured, but critical details may be obscured by broad class aggregation. We found a stronger alignment between DynamicWorld and ESRI Land Cover in the Forest and Other categories. ESA WorldCover also showed relatively good concordance with ESRI_LULC. Transition matrices showed major forest expansion in the Betsiboka basin, especially under SSP3 (+230%) and SSP5 (+300%) by 2100. Cropland is projected to increase under SSP4 and SSP5 (+100%) and decline under SSP1. Other land types are expected to decline (>−70%), converting to forest in all scenarios except SSP1, which shows more modest forest gains. This substantial decline in "Other" land types masks critical land cover transitions. Results demonstrated that the ANP showed short-term resilience but faces long-term vulnerability, even under sustainable pathways. The forest cover is projected to decline by −39.4% under SSP1–RCP26, −2.2% SSP5–RCP85, and −1.4%, SSP3–RCP70. No significant expansion of cropland is projected across all SSP scenarios. Importantly, these projections are uncertain scenarios, illustrating possibilities rather than forecasts amid Madagascar's deforestation. In Betsiboka basin, adaptive policies should balance forest recovery with the needs of local agriculture, whereas in ANP, sustained and adaptive forest management is essential to safeguard long-term ecological resilience. To strengthen the applicability of global LULC datasets in regional contexts, we recommend that policymakers integrate these datasets with local field data and national statistics to ensure context-appropriate decision-making. For researchers, it is important to cross-validate multiple products, select datasets suited to their spatial and thematic needs, and explicitly report uncertainties. For dataset developers, greater transparency in methods and co-production with local experts and monitoring initiatives will enhance both accuracy and regional relevance.

Author Contributions: Z.H.R.: Conceptualization, methodology, software, visualization, data analysis, writing—original draft, reviewing, and editing. N.O.: Supervision, validation, funding acquisition, writing—review, and editing. Z.M.H.R.: Conceptualization, data curating and analysis, writing—review and editing. All authors have read and agreed to the published version of the manuscript.

Funding: This research received grant funding from the JSPS International Research Fellow, Japan Grant Number JP25KF0059, Graduate School of Informatics, Kyoto University.

Data Availability Statement: The full Python implementation is available at https://doi.org/10.5281/zenodo.16598166 (accessed on 5 September 2025), enabling replication for other regions or datasets.

Acknowledgments: The authors extend their sincere gratitude to the editor and the anonymous reviewers for their valuable feedback.

Conflicts of Interest: The authors declare no conflicts of interest.

Appendix A

Confusion Matrices Comparing the Agreement Between Datasets

Figure A1 below presents a series of confusion matrices comparing the agreement between four global LULC datasets in the years 2017 and 2021. Each matrix compares two datasets across three generalized land cover classes: Forest, Cropland, and Other. The color

gradient reflects the logarithmic scale of agreement, with darker green indicating higher overlap in classification.

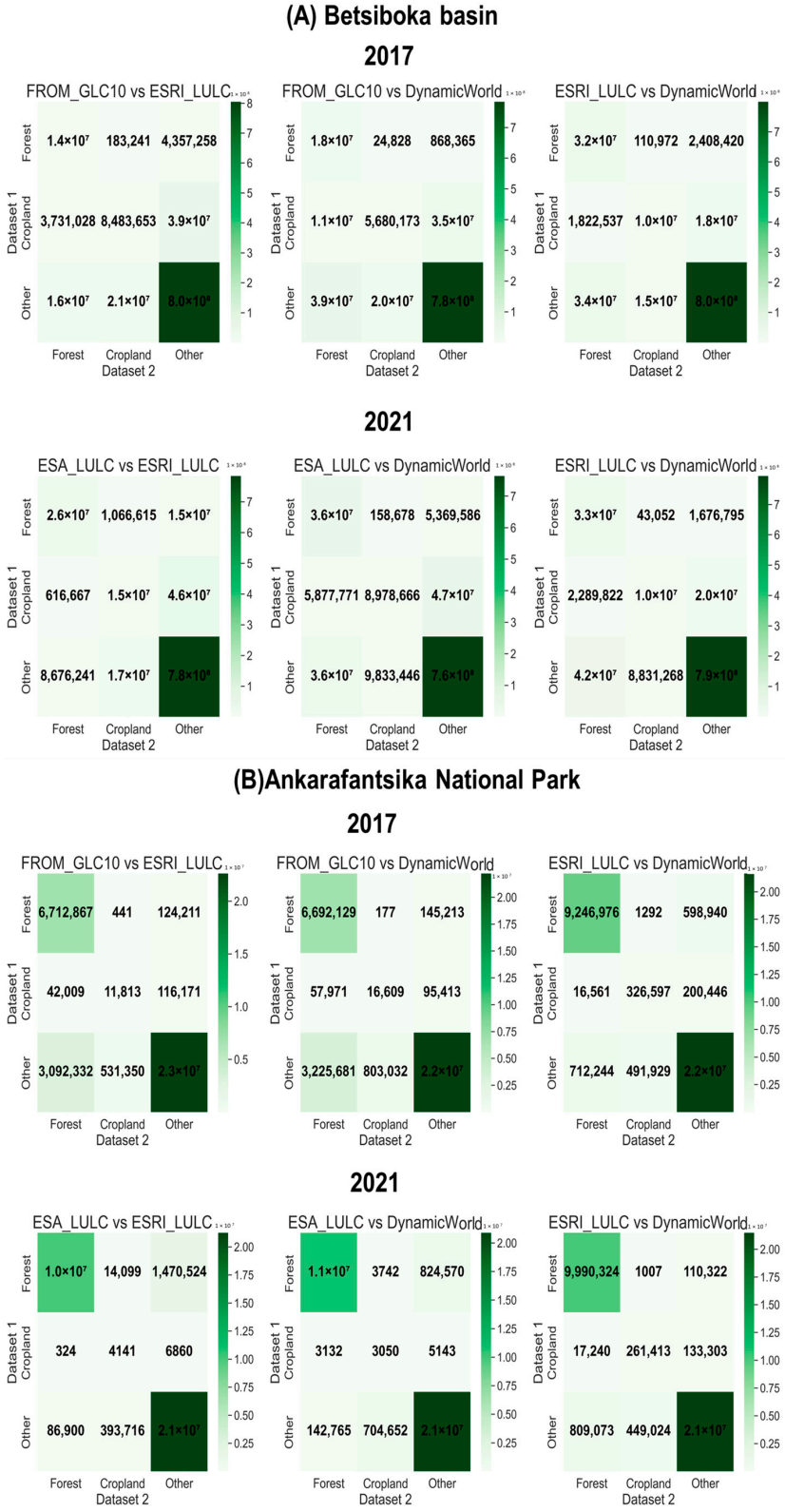


Figure A1. Confusion matrices comparing global LULC datasets across the Betsiboka basin (**A**) and ANP (**B**) for the years 2017 and 2021.

In the case of the Betsiboka basin, FROM_GLC10 and ESRI_LULC showed high agreement in the "Other" category (3.05×10^8) in 2017. The cropland (8.48×10^6) and forest

(1.42×10^7) showed more moderate overlap. FROM_GLC10 and DynamicWorld aligned strongly in cropland (5.68×10^7) and other (1.78×10^8), but less in forest (1.79×10^7). Similarly, ESRI_LULC and DynamicWorld shared strong agreements in cropland (1.03×10^8) and other (2.99×10^8), but lower overlap in forest (3.18×10^7). In 2021, ESA_LULC and ESRI_LULC matched closely in cropland (1.47×10^8) and others (2.83×10^8), with limited consistency in forest (2.56×10^7). ESA_LULC and DynamicWorld agreed most in Other (6.34×10^7) and cropland (4.67×10^7), but not in forest (3.62×10^7). ESRI_LULC and DynamicWorld also showed strong consistency in cropland (1.01×10^8) and Other (9.34×10^7), but weaker alignment in forest (3.32×10^7). Across both years, the "Other" class consistently demonstrated the highest agreement, followed by cropland with moderate to high overlap. Forest, however, showed the lowest consistency among all datasets, suggesting persistent challenges in forest classification. Notably, DynamicWorld aligned more closely with ESRI_LULC and FROM_GLC10, especially in non-forest classes.

Regarding the case of ANP, FROM_GLC10 and ESRI_LULC showed the highest agreement in the "Other" category (2.26×10^7), while agreement in Forest (6.71×10^6) and Cropland (1.18×10^4) was considerably lower in 2017. A similar trend appeared in the comparison between FROM_GLC10 and DynamicWorld, with the strongest match in "Other" (2.22×10^7), followed by Forest (6.69×10^6) and minimal alignment in Cropland (5.80×10^4). The ESRI_LULC and DynamicWorld comparison also indicated substantial consistency in "Other" (2.16×10^7) and Forest (9.25×10^6), but weak agreement in Cropland (3.27×10^5). In 2021, ESA_LULC and ESRI_LULC exhibited strong agreements in Forest (1.00×10^7) and "Other" (2.12×10^7), with very limited overlap in Cropland (3.94×10^5). ESA_LULC and DynamicWorld shared similar alignment in Forest (1.06×10^7) and "Other" (2.09×10^7), while Cropland agreement was again minimal (7.04×10^3). ESRI_LULC and DynamicWorld maintained high consistency in Forest (9.99×10^6) and "Other" (2.15×10^7) yet showed poor Cropland agreement (2.61×10^5). Across both years, the "Other" land cover class consistently showed the highest level of agreement among all dataset pairs, followed by Forest with moderate consistency. In contrast, Cropland exhibited the lowest levels of agreement, highlighting persistent discrepancies in its classification across global LULC products. Notably, DynamicWorld aligned more closely with ESRI_LULC in both forest and other classes, while ESA_LULC and ESRI_LULC also showed strong overlap in these categories but diverged considerably in Cropland.

Despite the scale difference, the patterns of the agreement are similar across the Betsiboka basin (up to 3×10^8) and ANP (up to 2×10^7). Across all datasets and time points, the "Other" land cover category showed the highest levels of agreement, while "Forest" exhibited moderate consistency and "Cropland" consistently revealed the lowest agreement. Notably, the alignment between DynamicWorld and ESRI_LULC was stronger, especially in the Forest and Other categories, with ESA_LULC also showing relatively good concordance with ESRI_LULC. Temporal comparisons indicated stable trends from 2017 to 2021, with persistent classification strengths and challenges across scales: "Other" remained reliably classified, Forest maintained moderate alignment, and Cropland posed ongoing inconsistencies. These findings emphasize the need for improved harmonization and validation strategies, particularly for cropland mapping, which appears to be the most variable and uncertain land cover class.

References

1. Rakotoarimanana, Z.H.; Ishidaira, H.; Magome, J.; Souma, K. Unveiling hydrological responses in Madagascar's major river basins: Addressing data scarcity and land-use change impacts. *Hydrol. Sci. J.* **2025**, *70*, 559–580. [CrossRef]
2. Talukdar, S.; Singha, P.; Mahato, S.; Pal, S.; Liou, Y.A.; Rahman, A. Land-use land-cover classification by machine learning classifiers for satellite observations—A review. *Remote Sens.* **2020**, *12*, 1135. [CrossRef]

3. Tyukavina, A.; Stehman, S.V.; Pickens, A.H.; Potapov, P.; Hansen, M.C. Practical global sampling methods for estimating area and map accuracy of land cover and change. *Remote Sens. Environ.* **2025**, *324*, 114714. [CrossRef]
4. He, D.; Shi, Q.; Xue, J.; Atkinson, P.M.; Liu, X. Very fine spatial resolution urban land cover mapping using an explicable sub-pixel mapping network based on learnable spatial correlation. *Remote Sens. Environ.* **2023**, *299*, 113884. [CrossRef]
5. Zanaga, D.; Van De Kerchove, R.; Daems, D.; De Keersmaecker, W.; Brockmann, C.; Kirches, G.; Wevers, J.; Cartus, O.; Santoro, M.; Fritz, S.; et al. ESA WorldCover 10 m 2021 v200 (Version v200) [Data set]. *Zenodo* **2022**. [CrossRef]
6. Karra, K.; Kontgis, C.; Statman-Weil, Z.; Mazzariello, J.C.; Mathis, M.; Brumby, S.P. Global land use/land cover with Sentinel-2 and deep learning. In Proceedings of the 2021 IEEE International Geoscience and Remote Sensing Symposium IGARSS, Brussels, Belgium, 11–16 July 2021; Volume 2021, pp. 4704–4707. [CrossRef]
7. Brown, C.F.; Brumby, S.P.; Guzder-Williams, B.; Birch, T.; Hyde, S.B.; Mazzariello, J.; Tait, A.M. Dynamic World: Near real-time global 10 m land use land cover mapping. *Sci. Data* **2022**, *9*, 251. [CrossRef]
8. Gong, P.; Liu, H.; Zhang, M.; Li, C.; Wang, J.; Huang, H.; Song, L. Stable classification with limited sample: Transferring a 30-m resolution sample set collected in 2015 to mapping 10-m resolution global land cover in 2017. *Sci. Bull.* **2019**, *64*, 370–373. [CrossRef]
9. Venter, Z.S.; Barton, D.N.; Chakraborty, T.; Simensen, T.; Singh, G. Global 10 m land use land cover datasets: A comparison of Dynamic World, WorldCover and ESRI land cover. *Remote Sens.* **2022**, *14*, 4101. [CrossRef]
10. Xu, P.; Tsendbazar, N.E.; Herold, M.; De Bruin, S.; Koopmans, M.; Birch, T.; Zanaga, D. Comparative validation of recent 10 m-resolution global land cover maps. *Remote Sens. Environ.* **2024**, *311*, 114316. [CrossRef]
11. Xu, Q.; Yordanov, V.; Bruzzone, L.; Brovelli, M.A. High-resolution global land cover maps and their assessment strategies. *ISPRS Int. J. Geo-Inf.* **2025**, *14*, 235. [CrossRef]
12. Zhai, J.; Xiao, C.; Feng, Z.; Liu, Y. Are there suitable global datasets for monitoring of land use and land cover in the tropics? Evidences from mainland Southeast Asia. *Glob. Planet. Change* **2023**, *229*, 104233. [CrossRef]
13. Kerner, H.; Nakalembe, C.; Yang, A.; Zvonkov, I.; McWeeny, R.; Tseng, G.; Becker-Reshef, I. How accurate are existing land cover maps for agriculture in Sub-Saharan Africa? *Sci. Data* **2024**, *11*, 486. [CrossRef]
14. Mudele, O.; Childs, M.L.; Personnat, J.; Golden, C.D. Evaluating agreement between global satellite data products for forest monitoring in Madagascar. *Remote Sens.* **2025**, *17*, 1482. [CrossRef]
15. Bullock, E.L.; Healey, S.P.; Yang, Z.; Oduor, P.; Gorelick, N.; Omondi, S.; Cohen, W.B. Three decades of land cover change in East Africa. *Land* **2021**, *10*, 150. [CrossRef]
16. Ngcofe, L.; Nkoana, K. Sentinel-2 land cover product comparison: South African National land cover 2020 vs ESRI Global land cover 2020. *Abstr. Int. Cartogr. Assoc.* **2023**, *6*, 186. [CrossRef]
17. Adam, A.Y.F.; Osman, M.B.O.; Gribovszki, Z.; Kalicz, P. Geospatial technologies' concepts and methods for land use land cover dynamics mapping: Evidence from White Nile State, Sudan. In *Application of Geospatial Technology and Modelling on Natural Resources Management*; Das, S., Pandey, P.C., Mutanga, O., Tikle, S., Jiang, M., Chatterjee, U., Anand, A., Eds.; Advances in Geographic Information Science; Springer: Cham, Switzerland, 2025. [CrossRef]
18. Li, Q.; Qiu, C.; Ma, L.; Schmitt, M.; Zhu, X.X. Mapping the land cover of Africa at 10 m resolution from multi-source remote sensing data with Google Earth Engine. *Remote Sens.* **2020**, *12*, 602. [CrossRef]
19. Zhang, M.; Huang, H.; Li, Z.; Hackman, K.O.; Liu, C.; Andriamiarisoa, R.L.; Gong, P. Automatic high-resolution land cover production in Madagascar using Sentinel-2 time series, tile-based image classification and Google Earth Engine. *Remote Sens.* **2020**, *12*, 3663. [CrossRef]
20. Carrasco, J.; Price, V.; Tulloch, V.; Mills, M. Selecting priority areas for the conservation of endemic trees species and their ecosystems in Madagascar considering both conservation value and vulnerability to human pressure. *Biodivers. Conserv.* **2020**, *29*, 1841–1854. [CrossRef]
21. Harper, G.J.; Steininger, M.K.; Tucker, C.J.; Juhn, D.; Hawkins, F. Fifty years of deforestation and forest fragmentation in Madagascar. *Environ. Conserv.* **2007**, *34*, 325–333. [CrossRef]
22. Vieilledent, G.; Grinand, C.; Rakotomalala, F.A.; Ranaivosoa, R.; Rakotoarijaona, J.R.; Allnutt, T.F.; Achard, F. Combining global tree cover loss data with historical national forest cover maps to look at six decades of deforestation and forest fragmentation in Madagascar. *Biol. Conserv.* **2018**, *222*, 189–197. [CrossRef]
23. Rasolofoson, R.A.; Ferraro, P.J.; Jenkins, C.N.; Jones, J.P.G. Effectiveness of community forest management at reducing deforestation in Madagascar. *Biol. Conserv.* **2015**, *184*, 271–277. [CrossRef]
24. Rafanoharana, S.C.; Andrianambinina, F.O.D.; Rasamuel, H.A.; Waeber, P.O.; Wilmé, L.; Ganzhorn, J.U. Projecting forest cover in Madagascar's protected areas to 2050 and its implications for lemur conservation. *Oryx* **2024**, *58*, 155–163. [CrossRef]
25. Raharimahefa, T.; Kusky, T.M. Environmental monitoring of Bombetoka Bay and the Betsiboka Estuary, Madagascar, using multi-temporal satellite data. *J. Earth Sci.* **2010**, *21*, 210–226. [CrossRef]
26. Rajaonarivelo, F.; Williams, R. Remote sensing-based land suitability analysis for forest restoration in Madagascar. *Forests* **2022**, *13*, 1727. [CrossRef]

27. Sato, H. Significance of seed dispersal by the largest frugivore for large-diaspore trees. *Sci. Rep.* **2022**, *12*, 19086. [CrossRef]
28. Dumas, D.; Bigot, S.; Brou, Y.T.; Ramboarison, R.; Razanaka, S.; Robison, L.R. Evolution des apports en eau dans la plaine rizicole de Marovoay par le fleuve Betsiboka (Madagascar): Reconstitution et projections jusqu'en 2100. *Proc. Int. Assoc. Hydrol. Sci.* **2021**, *384*, 175–179. [CrossRef]
29. Rakotoarimanana, Z.H.; Ishidaira, H.; Rakotoarimanana, Z.M.H.; Magome, J.; Souma, K.; Masutani, K. Assessing future intra-basin water availability in Madagascar: Accounting for climate change, population growth, and land use change. *Water Res.* **2024**, *257*, 121711. [CrossRef] [PubMed]
30. Percival, J.E.H.; Sato, H.; Razanaparany, T.P.; Rakotomamonjy, A.H.; Razafiarison, Z.L.; Kitajima, K. Non fire-adapted dry forest of Northwestern Madagascar: Escalating and devastating trends revealed by Landsat time series and GEDI lidar data. *PLoS ONE* **2024**, *19*, e0290203. [CrossRef]
31. Rasolozaka, M.; Schüßler, D.; Randriafenontsoa, J.; Andriatsitohaina, F.; Rakotomamonjy, P.; Rabarison, H.; Radespiel, U. Reconstructing the alarming fire history of Ankarafantsika National Park in northwestern Madagascar over a 35-year period. *Remote Sens. Appl. Soc. Environ.* **2025**, *38*, 101521. [CrossRef]
32. Ralimanana, H.; Perrigo, A.L.; Smith, R.J.; Borrell, J.S.; Faurby, S.; Rajaonah, M.T.; Antonelli, A. Madagascar's extraordinary biodiversity: Threats and opportunities. *Science* **2022**, *378*, eadf1466. [CrossRef]
33. Zhang, T.; Cheng, C.; Wu, X. Mapping the spatial heterogeneity of global land use and land cover from 2020 to 2100 at a 1 km resolution. *Sci. Data* **2023**, *10*, 748. [CrossRef]
34. Barati, A.A.; Zhoolideh, M.; Azadi, H.; Lee, J.H.; Scheffran, J. Interactions of land-use cover and climate change at a global level: How to mitigate the environmental risks and warming effects. *Ecol. Indic.* **2023**, *146*, 109829. [CrossRef]
35. Mondanaro, A.; Di Febbraro, M.; Castiglione, S.; Belfiore, A.M.; Girardi, G.; Melchionna, M.; Raia, P. Modelling reveals the effect of climate and land use change on Madagascar's chameleons fauna. *Commun. Biol.* **2024**, *7*, 889. [CrossRef]
36. Lai, Q.; Beierkuhnlein, C. The vulnerability of Malagasy protected areas in the face of climate change. *Diversity* **2024**, *16*, 661. [CrossRef]
37. Ding, Y.; Yang, X.; Wang, Z.; Fu, D.; Li, H.; Meng, D.; Zhang, J. A field-data-aided comparison of three 10 m land cover products in Southeast Asia. *Remote Sens.* **2022**, *14*, 5053. [CrossRef]
38. Minten, B.; Barrett, C.B. Agricultural technology, productivity, and poverty in Madagascar. *World Dev.* **2008**, *36*, 797–822. [CrossRef]
39. Zaehringer, J.G.; Eckert, S.; Messerli, P. Revealing regional deforestation dynamics in North-Eastern Madagascar—Insights from multi-temporal land cover change analysis. *Land* **2015**, *4*, 454–474. [CrossRef]
40. Liang, S.; He, T.; Huang, J.; Jia, A.; Zhang, Y.; Cao, Y.; Song, L. Advancements in high-resolution land surface satellite products: A comprehensive review of inversion algorithms, products and challenges. *Sci. Remote Sens.* **2024**, *10*, 100152. [CrossRef]
41. Andriatsitohaina, R.N.N.; Laby, P.; Llopis, J.C.; Martin, D.A. Agroforestry in Madagascar: Past, present, and future. *Agrofor. Syst.* **2024**, *98*, 1659–1680. [CrossRef]
42. Weiskopf, S.R.; Cushing, J.A.; Morelli, T.L.; Myers, B.J. Climate change risks and adaptation options for Madagascar. *Ecol. Soc.* **2021**, *26*, 36. [CrossRef]
43. Andrianandrasana, H.T.; Jones, N.; Viraina, F.F.; Malesios, C.; Campera, M.; Zefania, S.; Savage, J. Links between poverty, climate-induced migration and deforestation in western Madagascar. *Environ. Dev.* **2025**, *56*, 101284. [CrossRef]

Disclaimer/Publisher's Note: The statements, opinions and data contained in all publications are solely those of the individual author(s) and contributor(s) and not of MDPI and/or the editor(s). MDPI and/or the editor(s) disclaim responsibility for any injury to people or property resulting from any ideas, methods, instructions or products referred to in the content.